

Supporting Information

Temperature stable $\text{Sm}(\text{Nb}_{1-x}\text{V}_x)\text{O}_4$ ($0.0 \leq x \leq 0.9$) microwave dielectric ceramics with ultra-low dielectric loss for dielectric resonator antenna applications

Fangfang Wu,^a Di Zhou,^{*a} Chao Du,^a Shikuan Sun,^b Lixia Pang,^c Biaobing Jin,^d Zeming Qi,^e Jobin Varghese,^f Qiang Li,^g and Xiuqun Zhang^h

^aKey Laboratory of Multifunctional Materials and Structures, Ministry of Education, School of Electronic Science and Engineering, Xi'an Jiaotong University, Xi'an 710049, Shaanxi, China

^aKey Laboratory of Multifunctional Materials and Structures, Ministry of Education, School of Electronic Science and Engineering, Xi'an Jiaotong University, Xi'an 710049, Shaanxi, China

^bSchool of Material Science and Energy Engineering, Foshan University, Foshan, Guangdong, 528000 PR China

^cMicro-optoelectronic Systems Laboratories, Xi'an Technological University, Xi'an 710032, Shaanxi, China

^dResearch Institute of Superconductor Electronics (RISE), School of Electronic Science and Engineering, Nanjing University, Nanjing, Jiangsu, 210093, China.

^eNational Synchrotron Radiation Laboratory, University of Science and Technology of China, Hefei, China

^fHybrid Microsystems, Fraunhofer Institute for Ceramic Technology and Systems IKTS, Winterbergstr 28, 01277 Dresden, Germany

^gZTE Corporation, District Nanshan, Shenzhen, 518000, China

^hZTE Corporation, District Yuhuatai, Nanjing, 210012, China

*Corresponding Author: E-mail: zhoudi1220@gmail.com (Di Zhou)

Experimental

The $\text{Sm}(\text{Nb}_{1-x}\text{V}_x)\text{O}_4$ ($0 \leq x \leq 0.9$) ceramics were synthesized by conventional solid-state reaction, and the raw materials were the high-purity powders of Sm_2O_3 (99.9%), Nb_2O_5 (99.99%) and V_2O_5 (99%). All the materials were weighed according to the stoichiometric formulation of $\text{Sm}(\text{Nb}_{1-x}\text{V}_x)\text{O}_4$ ($0 \leq x \leq 0.9$), and Sm_2O_3 powder was calcined at 1200 °C for 4 h before weighting. Then, these powders were mixed with zirconia balls and ethanol in a certain proportion and milled for 4 h. The powder mixtures were rapidly dried and calcined at 1000 - 1150 °C for 4 h, and the calcined powder was ball-milled in ethanol for 5 h. Finally, the dried powders were granulated with 5 wt% polyvinyl alcohol adhesive (PVA) and pressed into a cylindrical mold to obtain several samples (10 mm in diameter and 4-5 mm in height). Samples were sintered at 1150 - 1520 °C for 3 h.

The phase purity of the samples was investigated using room-temperature X-ray diffraction (XRD) with Cu K α radiation (Rigaku D/MAX-2400 X-ray diffractometry, Tokyo, Japan). The Rietveld profile refinement method was employed to analyze the crystal structure of ceramics using GSAS program and the diffraction pattern was obtained with 2 θ in the range of 10°-120°. Shrinkage value of the sample was measured with a horizontal-loading dilatometer with alumina rams and boats (DIL 402C, Netzsch Instruments, Germany) with different heating rate of 5, 10 and 15K / min from ambient temperature to 1000 °C, respectively. The high-resolution transmission electron microscopy (HRTEM) and selected area electron diffraction (SAED) patterns measurements were measured on JEM-2100 with an accelerating voltage of 200 kV. The microstructures and energy-dispersive spectroscopy (EDS) of the sintered specimens were observed by electron scanning microscopy (SEM; Quanta 250, FEI). The mean grain size was calculated from each SEM image of the $\text{SmNb}_{1-x}\text{V}_x\text{O}_4$ ($0 \leq x \leq 0.9$) ceramics using image analysis software (Nano Measurer 1.2). The room-temperature Raman spectra were performed with a Laser Raman Spectrometer of the natural surface of samples and acquired with a 532 nm laser excitation source. The room temperature infrared reflectivity spectra were measured using a Bruker IFS 66v FT-IR spectrometer on infrared beamline station (U4) at National Synchrotron Radiation Lab (NSRL), China. The microwave dielectric properties were measured with the TE₀₁₆ dielectric resonator method with a network analyzer (8720ES, Agilent, Palo Alto, CA) and a temperature

*Corresponding author E-mail address: zhoudi1220@gmail.com (Di Zhou)

chamber (Delta 9023, Delta Design, Poway, CA). The temperature coefficient of resonant frequency (*TCF*) was measured in the temperature range from 25 - 85 °C. The temperature coefficient of resonant frequency (*TCF*) was calculated by the following formula:

$$TCF = \frac{f_T - f_{T_0}}{f_{T_0}(T - T_0)} \times 10^6$$

where, f_T and f_{T_0} were the TE₀₁₆ resonant frequencies at temperature T and T_0 , respectively. Finally, the RDRA antenna of SNV-0.2 ceramic is designed and simulated by the CST Microwave Studio 2019® software, and the return loss S_{11} of RDRA antenna was measured by microwave network analyzer.

Table S1. Microwave dielectric properties of ReNbO₄-based (Re = La, Nd, Sm) compounds

	ϵ_r	$Q \times f$ (GHz)	<i>TCF</i> (ppm/°C)	Ref.
NdNbO ₄ -0.6CaTiO ₃	18.21	70,000	-31.1	1
LaNbO ₄ -0.5MgO	19.80	94,440	+6.1	2
Nd _{0.9} Zn _{0.1} NbO _{4-0.1/2}	18.53	60,000	-43.9	3
(Nd _{0.97} Mn _{0.045}) _{1.02} Nb _{0.988} O ₄	19.81	80,000	-23.2	4
(Nd _{0.92} Y _{0.08})NbO ₄	19.87	81,100	-18.84	5
(Nd _{0.92} Sm _{0.08})NbO ₄	19.56	66,200	-28.37	6
(Nd _{0.94} La _{0.06})NbO ₄	21.52	46,600	0	7
(Nd _{0.94} Yb _{0.06})NbO ₄	20.88	66,510	-36.59	8
(Nd _{0.9} Bi _{0.1})NbO ₄	22.5	50,000	-9	9
La(Nb _{0.92} Ta _{0.08})NbO ₄	19.23	65,653	+3.03	10
Nd(Nb _{0.92} Sb _{0.08})O ₄	20.06	73,200	-23.1	11
La(Nb _{0.7} V _{0.3})O ₄	17.78	75,940	-36.8	12
NdNb _{0.96} (Zr _{0.5} W _{0.5}) _{0.04} O ₄	19.2	55,282	-11.36	13
NdNb _{0.96} (Mg _{1/4} W _{3/4}) _{0.04} O ₄	19.59	50,339	-39.62	14
NdNb _{0.96} (Al _{1/3} W _{2/3}) _{0.04} O ₄	19.04	58,219	-41.14	15
0.85CaWO ₄ -0.15SmNbO ₄	11.6	61,000	-25	16
SmNb _{0.31} (Si _{1/2} Mo _{1/2}) _{0.69} O ₄	15.6	32,800	-38.2	17
SmNbO ₄ -4MgO	14.12	182,400	unkown	18

Table S2. Room-temperature crystal structure of Re(Nb_{1-x}V_x)O₄ (Re = La, Ce, Nd) compounds

LaNb _{1-x} V _x O ₄ ¹⁹		CeNb _{1-x} V _x O ₄ ²⁰		NdNb _{1-x} V _x O ₄ ²⁰		SmNb _{1-x} V _x O ₄ ^[this paper]	
x	Structure	x	Structure	x	Structure	x	Structure
0	Fergusonite	0	Fergusonite	0	Fergusonite	0	Fergusonite
0.248	Scheelite	0.300	Scheelite	0.350	Scheelite	0.300	Fergusonite + Zircon
0.895	Monazite	0.975	Zircon	0.972	Zircon	0.900	Zircon
1.0		1.0		1.0		1.0	Zircon

Table S3. Crystallographic parameters of different x values of the Sm(Nb_{1-x}V_x)O₄ (0 ≤ x ≤ 0.4) ceramics

x	atom	x	y	z	occupancy	mult
0	Sm1	0.2500	0.6211	0.0000	1.0000	4
	Nb1	0.2500	0.1459	0.0000	1.0000	4
	O1	0.0975	0.4576	0.2562	1.0000	8
	O2	-0.0084	0.7180	0.2927	1.0000	8
0.1	Sm1	0.2500	0.6211	0.0000	1.0000	4
	Nb1	0.2500	0.1459	0.0000	0.9000	4
	V1	0.2500	0.1459	0.0000	0.1000	4
	O1	0.0975	0.4576	0.2562	1.0000	8
	O2	-0.0084	0.7180	0.2927	1.0000	8
0.2	Sm1	0.2500	0.6211	0.0000	1.0000	4
	Nb1	0.2500	0.1459	0.0000	0.8000	4
	V1	0.2500	0.1459	0.0000	0.2000	4
	O1	0.0975	0.4576	0.2562	1.0000	8
	O2	-0.0084	0.7180	0.2927	1.0000	8
0.3	Sm1	0.2500	0.6211	0.0000	1.000	4
	Nb1	0.2500	0.1459	0.0000	0.7000	4
	V1	0.2500	0.1459	0.0000	0.3000	4
	O1	0.0975	0.4576	0.2562	1.0000	8
	O2	-0.0084	0.7180	0.2927	1.0000	8
0.4	Sm1	0.2500	0.6228	0.0000	1.0000	4
	Nb1	0.2500	0.1364	0.0000	0.6000	4
	V1	0.2500	0.1364	0.0000	0.4000	4
	O1	0.0967	0.4623	0.2706	1.0000	8
	O2	-0.0230	0.7166	0.3309	1.0000	8

Table S4. Bond Length d from Rietveld Refinement for the $\text{Sm}(\text{Nb}_{1-x}\text{V}_x)\text{O}_4$ ($0.1 \leq x \leq 0.4$) ceramics

bond type	x = 0	x = 0.1	x = 0.2	x = 0.3	x = 0.4
Sm-O (1) $\times 2$	2.375	2.382	2.390	2.398	2.443
Sm-O (1) $\times 2$	2.433	2.431	2.428	2.426	2.464
Sm-O (2) $\times 2$	2.392	2.378	2.361	2.345	2.461
Sm-O (2) $\times 2$	2.466	2.474	2.483	2.493	2.506
Nb/V-O (1) $\times 2$	1.847	1.856	1.866	1.878	1.800
Nb/V-O (2) $\times 2$	1.928	1.915	1.899	1.883	1.758
Nb/V-O (2) $\times 2$	2.440	2.451	2.463	2.477	2.643

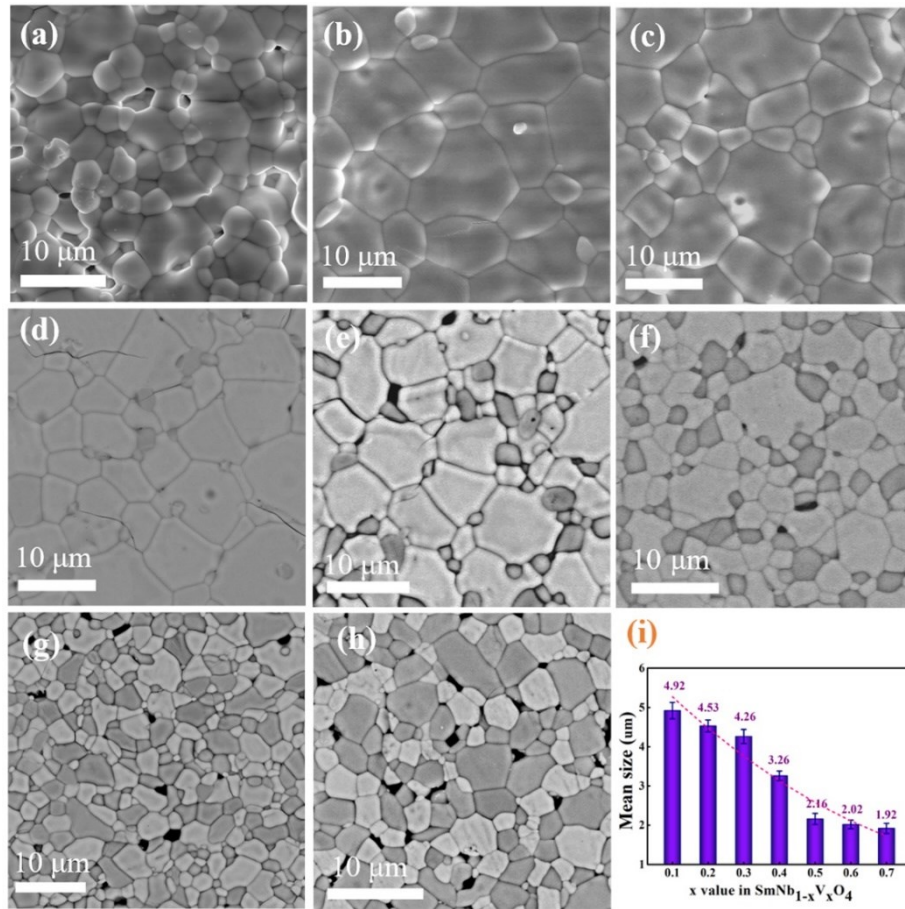


Figure S4. SEM images of the $\text{Sm}(\text{Nb}_{1-x}\text{V}_x)\text{O}_4$ ($0 \leq x \leq 0.2$) ceramics, BSEI of polished surface of the SNV-x ($0.3 \leq x \leq 0.7$).

Table S6. The phonon parameters obtained by fitting the infrared reflection spectrum of the $\text{Sm}(\text{Nb}_{1-x}\text{V}_x)\text{O}_4$ ($0.2 \leq x \leq 0.4$) ceramics.

mode	x=0.2				x=0.3				x=0.4			
	ω_{oj}	ω_{pj}	γ_j	$\Delta\epsilon_j$	ω_{oj}	ω_{pj}	γ_j	$\Delta\epsilon_j$	ω_{oj}	ω_{pj}	γ_j	$\Delta\epsilon_j$
1	129.42	411.97	37.62	10.100	135.22	138.08	20.04	1.040	134.28	125.99	17.87	0.880
2	154.17	246.94	18.89	2.570	157.41	237.26	21.55	2.270	159.31	282.17	29.81	3.140
3	194.46	277.20	26.50	2.030	199.29	335.68	41.35	2.840	197.43	343.51	40.30	3.030
4	244.77	74.98	20.96	0.090	259.59	206.24	71.76	0.630	239.62	199.47	49.01	0.690
5	269.49	159.55	33.91	0.350	340.64	95.76	14.48	0.080	268.58	129.18	31.55	0.230
6	335.89	398.11	70.41	1.400	359.07	273.61	38.83	0.580	355.11	315.80	50.60	0.790
7	358.97	45.66	8.53	0.020	460.99	230.18	33.34	0.250	460.00	244.34	39.78	0.280
8	442.66	316.84	56.97	0.510	515.60	93.35	22.20	0.030	515.68	86.81	22.15	0.030
9	508.25	221.30	40.18	0.190	616.82	214.01	23.48	0.120	622.78	362.49	30.46	0.340
10	551.63	274.40	52.37	0.250	648.84	745.88	76.65	1.320	651.63	588.33	42.89	0.820
11	587.95	318.40	51.41	0.290	655.41	117.06	20.55	0.030	678.72	386.53	51.53	0.320
12	633.22	230.75	54.66	0.130	722.52	328.39	60.49	0.210	720.65	525.79	67.26	0.530
13	717.86	139.84	85.42	0.040	806.36	138.71	44.21	0.030	802.26	183.00	57.91	0.050
14	793.29	85.36	38.85	0.010	860.85	49.03	22.76	0.003	860.16	102.88	38.34	0.010
$\epsilon_\infty = 2.21$		$\epsilon_o = 20.24$		$\epsilon_\infty = 3.59$		$\epsilon_o = 13.10$		$\epsilon_\infty = 4.20$		$\epsilon_o = 15.37$		

References

1. P. Zhang, Z. K. Song, Y. Wang, Y. M. Han, H. L. Dong and L. X. Li, *J. Alloy. Compd.*, 2013, **581**, 741-746.
2. T. L. Tang, W. S. Xia, B. Zhang, Y. Wang, M. X. Li and L. W. Shi, *J. Materi. Sci.-Mater. EL*, 2019, **30**, 15293-15298.
3. Y. H. Chen, H. Wang, L. X. Pang, H. F. Zhou and X. Yao, *Ferroelectrics*, 2010, **407**, 61-68.
4. Z. K. Song, P. Zhang, Y. Wang and L. X. Li, *J. Alloy. Compd.*, 2014, **583**, 546-549.
5. Y. G. Zhao and P. Zhang, *RSC Adv.*, 2015, **5**, 97746-97754.
6. P. Zhang and Y. Zhao, *J. Alloy. Compd.*, 2016, **654**, 240-245.
7. P. Zhang, Y. Zhao and L. Li, *Phys. Chem. Chem. Phys.*, 2015, **17**, 16692-16698.
8. Y. G. Zhao and P. Zhang, *Ceram. Int.*, 2018, **44**, 1935-1941.
9. L. X. Pang and D. Zhou, *J. Am. Ceram. Soc.*, 2019, **102**, 2278-2282.
10. M. Xiao, Y. S. Wei, Q. Q. Gu, Z. Q. Zhou and P. Zhang, *J. Alloy. Compd.*, 2019, **775**, 168-174.
11. P. Zhang, Y. G. Zhao and X. Y. Wang, *Dalton T.*, 2015, **44**, 10932-10938.
12. D. Guo, D. Zhou, W. B. Li, L. X. Pang, Y. Z. Dai and Z. M. Qi, *Inorg. Chem.*, 2017, **56**, 9321-9329.
13. H. C. Yang, S. R. Zhang, H. Y. Yang, Y. Yuan and E. Z. Li, *Ceram. Int.*, 2019, **45**, 16940-16947.
14. H. C. Yang, S. R. Zhang, H. Y. Yang, Y. Yuan and E. Z. Li, *J. Alloy. Compd.*, 2019, **787**, 358-366.
15. H. C. Yang, S. R. Zhang, H. Y. Yang, Y. Yuan and E. Z. Li, *Dalton T.*, 2018, **47**, 15808-15815.
16. S. J. Kim and E. S. Kim, *Ceram. Int.*, 2009, **35**, 137-141.
17. S. D. Ramarao and V. R. K. Murthy, *Phys. Chem. Chem. Phys.*, 2015, **17**, 12623-12633.
18. W. S. Xia, S. B. Zhang, T. L. Tang, Y. Wang and L. W. Shi, *Physica B: Condensed Matter.*, 2019, **572**, 148-152.
19. A. T. Aldred, *Mater. Lett.*, 1983, **1**, 197-199.
20. A. T. Alared, *J. Solid State Chem.*, 1985, **59**, 95-102.